PROCEEDINGS OF SCIENCE

Exploiting HI surveys with stacking. The HI content of massive galaxies from ALFALFA and GASS

Silvia Fabello*
Max-Planck Institut für Astrophysik, D-85741 Garching, Germany
E-mail: fabello@mpa-garching.mpg.de

Barbara Catinella
Max-Planck Institut für Astrophysik, D-85741 Garching, Germany
E-mail: bcatinel@mpa-garching.mpg.de

Guinevere Kauffmann
Max-Planck Institut für Astrophysik, D-85741 Garching, Germany
E-mail: gamk@mpa-garching.mpg.de

Riccardo Giovanelli
Center for Radiophysics and Space Research, Cornell University, Ithaca, NY 14853, USA
E-mail: riccardo@astro.cornell.edu

Martha P. Haynes
Center for Radiophysics and Space Research, Cornell University, Ithaca, NY 14853, USA
E-mail: haynes@astro.cornell.edu

David Schiminovich
Department of Astronomy, Columbia University, New York, NY 10027, USA
E-mail: ds@astro.columbia.edu

PoS(ISKAF2010)016

PROCEEDINGS OF SCIENCE

We have carried out an HI stacking analysis of a volume-limited sample of ~ 5000 galaxies with imaging and spectroscopic data from GALEX and the Sloan Digital Sky Survey. The galaxies have stellar masses greater than $10^{10} M_{\odot}$ and redshifts in the range $0.025 < z < 0.05$. We extract a sub-sample of 1833 "early-type" galaxies with inclinations less than 70°, with concentration indices $C > 2.6$ and with light profiles that are well fit by a De Vaucouleurs model. We then stack Arecibo Legacy Fast ALFA (ALFALFA) spectra of the galaxies from these two samples in bins of stellar mass, stellar mass surface density, central velocity dispersion, and NUV-*r* colour. We use the stacked spectra to estimate the average HI gas fractions HI/M_{*} of the galaxies in each bin. Our main result is that the HI content of a galaxy is not influenced by its bulge. The average HI gas fractions of galaxies in both our samples correlate most strongly with NUV-*r* colour and with stellar surface density. The relation between average HI fraction and these two parameters is independent of concentration index *C*, and hence of the bulge-to-disk ratio of the galaxy. We have also tested whether the average HI gas content of bulge-dominated galaxies on the red sequence, differs from that of late-type galaxies on the red sequence. We find no evidence that galaxies with a significant bulge component are less efficient at turning their available gas reservoirs into stars. This result is in contradiction with the "morphological quenching" scenario proposed by Martig et al. (2009).

ISKAF2010 Science Meeting - ISKAF2010
June 10-14, 2010
Assen, the Netherlands

*Speaker.

PoS(ISKAF2010)016

1. Introduction

Galaxies have long been known to follow well-ordered sequences in many properties. Irrespective of the exact classification scheme there are clear systematic trends which vary from spirals to ellipticals. With the advent of large spectroscopic surveys of nearby galaxies, such as the Sloan Digital Sky Survey (SDSS; [1]), the relationships between galaxy properties that can be derived from the combination of optical imaging and spectroscopy, e.g. stellar mass, size, concentration index, star formation rate, metallicity, dust content, have been studied and quantified in considerable detail. Our understanding of how the neutral gas content of galaxies relates to other galaxy properties lags far behind. If the cold gas content of a galaxy is known to vary strongly with colour and star formation rate, the connection between gas content and galaxy morphological type remains unclear. Whereas star-forming spiral galaxies almost always contain HI gas, the HI content of early-type galaxies is considerably more difficult to predict. Because early-type galaxies are more difficult to detect at 21 cm on average, the samples discussed in the literature have generally been quite small. First studies suggested that the cold gas in early-types is associated mainly with disks and not with the bulge components of these galaxies. However, more recent studies that have mapped HI in nearby early-type galaxies ([2]) have concluded that the HI can be organized in a variety of different configurations, e.g. in regular disks, in clouds, in rings, or even in tidal tail-like structures.

One major problem that has plagued our understanding of cold gas in early-type galaxies is that the available HI data have been inhomogeneous. Large area, blind HI surveys such as the Arecibo Legacy Fast ALFA Survey (ALFALFA; [3]) offer uniform coverage over large regions of the sky and allow one to construct complete, unbiased samples of HI-selected galaxies. However, these surveys are shallow, and do not in general detect gas-poor early-type galaxies.
Another problem has to do with the Hubble classification system itself. The position of a galaxy in the Hubble sequence depends on its *visual appearance* at optical wavelengths. In practice, the visual appearance of a galaxy depends both on structural properties such as its bulge-to-disk ratio, and on star formation rate. If we wish to understand the physical processes that regulate the neutral gas content of galaxies, it is preferable to analyze the effects of star formation and galaxy structure *separately*.

Here, we make use of stacking techniques to analyze whether the average HI gas fraction of a galaxy is affected or not by the presence of a significant bulge component. Stacking has now become a common tool to constrain the statistical properties of a population of objects that lack individual detections in a survey; by co-adding the signal from many objects with known sky position and redshift, the background noise can be decreased and one can recover the average HI flux of the population.
We use ALFALFA survey data to constrain the average HI gas fractions of an unbiased sample of massive early-type galaxies. We study how the HI content depends on parameters such as stellar mass, stellar mass surface density, concentration index, central velocity dispersion and UV/optical colour.

All distance-dependent quantities in this work are computed assuming $\Omega_m = 0.3$, $\Lambda = 0.7$ and $H_0 = 70$ km s^{-1} Mpc^{-1}.

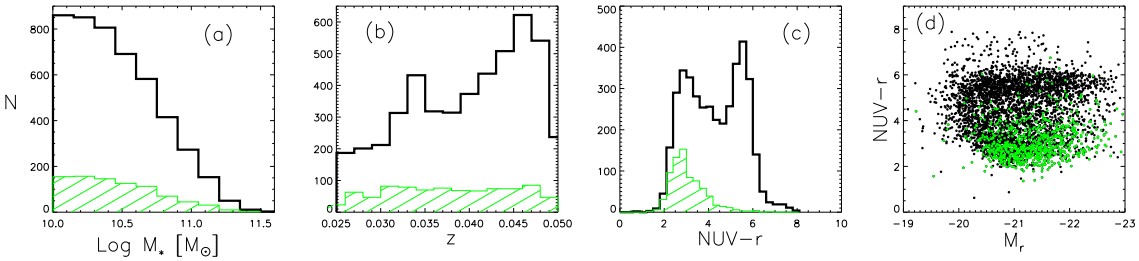

Figure 1: Distributions of (a) stellar mass, (b) redshift and (c) NUV-*r* colour (corrected for Galactic extinction only) for galaxies in *sample A*. The black solid histograms represent the whole sample, while the green, dashed histograms show the distributions for the galaxies with ALFALFA detections. Panel (d) shows the colour-magnitude diagram of *sample A* galaxies (black dots) and the sub-sample with ALFALFA detections (green dots).

2. Samples selection

Our sample is drawn from the "parent sample" of the GALEX Arecibo SDSS Survey (hereafter GASS-1; [4]), which is a sample of 12006 galaxies with stellar masses greater than $10^{10}M_{\odot}$ and redshifts in the range $0.025 < z < 0.05$ selected from the SDSS main spectroscopic sample. The parent sample galaxies are located in the intersection of the footprints of the Data Release 6 of the SDSS (DR6; [5]), the projected GALEX Medium Imaging Survey (MIS; [6]) and ALFALFA (dataset to be released in late 2010). They lie in the following SDSS sky regions: $7.5\,\mathrm{h} < \alpha_{2000} < 16.5\,\mathrm{h},\ +4^{\circ} < \delta_{2000} < +16^{\circ}$ and $+24^{\circ} < \delta_{2000} < +28^{\circ}$, and $22\,\mathrm{h} < \alpha_{2000} < 3\,\mathrm{h},\ +14^{\circ} < \delta_{2000} < +16^{\circ}$.

After cross-matching with the GASS parent sample a sample of 4726 galaxies remains. We call this massive galaxies sample: *sample A*. Of these, 23% are galaxies with reliable ALFALFA detections (i.e. objects corresponding to ALFALFA detection codes 1 or 2[1]. Panels (a), (b) and (c) of Figure 1 show the stellar mass, redshift and NUV-*r* colour distributions of the galaxies in *sample A*. The NUV-r colours have been corrected for foreground Galactic extinction, but not for internal extinction. The ALFALFA detection rate is close to 23% for each stellar mass bin, but is clearly biased to blue-sequence objects. In panel (d) we plot NUV-*r* colour versus absolute *r*-band magnitude M_r for the sample, with black dots representing the full sample and green points the galaxies detected by ALFALFA.

From the parent *sample A*, we cut our early-type sample. In this work, we have chosen to define "early-type" galaxies purely in terms of their structural properties, without regard to their stellar populations or star formation rates. We note that our definition is in contrast to some definitions of "early-types" in the literature, which have excluded galaxies with emission lines (e.g., [7, 8]). Our goal will be to explore the extent to which the presence or absence of a significant bulge component influences the HI content of a galaxy, so we do not wish to bias our conclusions by selecting against bulge-dominated galaxies with emission lines.

Starting from *sample A*, we extracted a subset of early-type objects (*ETG sample*) with the

[1]Code 1 detections have a peak signal-to-noise ratio greater than 6.5 and are reliable at greater than 95% confidence; Code 2 detections, referred to as "priors", have a lower signal-to-noise ratio between 4.5 and 6.5 but an optical counterpart at the same known redshift. Their reliability is estimated to be greater than 85%.

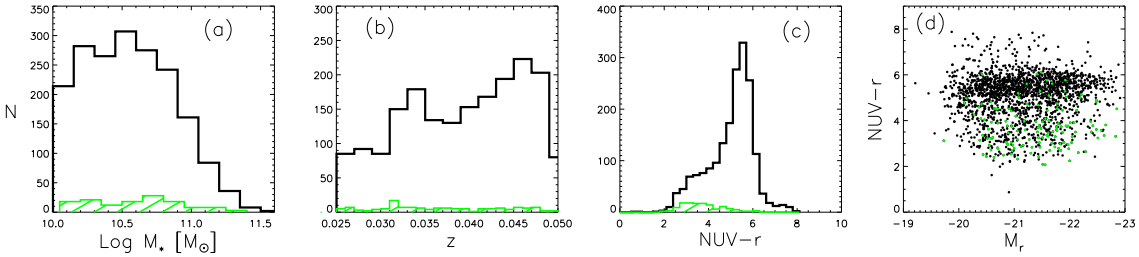

Figure 2: As in Figure 1, except for the *ETG sample*.

following properties: *i)* concentration index C=$R_{90}/R_{50} \geq 2.6$; *ii)* the likelihood that the light profile is fitted by a de Vaucouleurs model is greater than it is by an exponential one; *iii)* inclination less than 70° (this cut rejects the most inclined systems).

We note that the C parameter has been shown to be an excellent indicator of the bulge-to-total ratio derived from full 2-dimension bulge/disk decomposition analysis [9]. A cut at $C \geq 2.6$ restricts the sample to galaxies with $B/T \simeq 0.4$.

Our default cuts lead to an *ETG sample* consisting of 1833 objects. The properties of this sample are shown in Figure 2, where the panels and symbols are the same as in Fig. 1. The average ALFALFA detection rate for early-type objects is smaller ($\sim$ 9%) than for *sample A*. Most of the early-type targets lie on a well-defined red sequence. Some objects do scatter bluewards of the red sequence. Such objects may be star-forming, transitional or Seyfert galaxies. By selecting targets based on concentration index and inclination, we may also include objects with some disk component, as shown in Figure 3. There, we show SDSS postage stamps of a randomly selected set of galaxies from our *ETG sample*. The size of each stamp image is 1x1 arcminute.

The optical parameters we will use for the analysis are derived from the MPA-JHU SDSS DR7 release of spectrum measurements or from Structured Query Language (SQL) queries to the SDSS DR7 database server[2]. The UV parameters are extracted from the GALEX UV photometry by [10]. The reader is referred to section 5 of GASS-1 for more detailed descriptions.

3. ALFALFA data stacking

In the following section we briefly summarize the stacking technique we used; we remind the reader to [11] for further details.

ALFALFA will scan 7000 deg^2 of the sky over the velocity interval $v[\mathrm{km\,s^{-1}}] \simeq$[-2500;18000] (i.e. out to z$\sim$0.06). The data acquired are stored as smaller three dimensional cubes of dimension $2.4^\circ \times 2.4^\circ$ on the sky and 5500 $\mathrm{km\,s^{-1}}$ in velocity "depth". We refer the reader to Figure 4, where a schematic representation of one such data-cube is shown, for the details. We will refer to this picture throughout the paper.

The stacking process includes many steps, that we can summarize as follow:

a. Creating a catalogue of HI spectra

All our targets are selected from the SDSS spectroscopic survey, so we know their positions on the

[2]See http://www.mpa-garching.mpg.de/SDSS/DR7/ and http://cas.sdss.org./dr7/en/tools/search/sql.asp

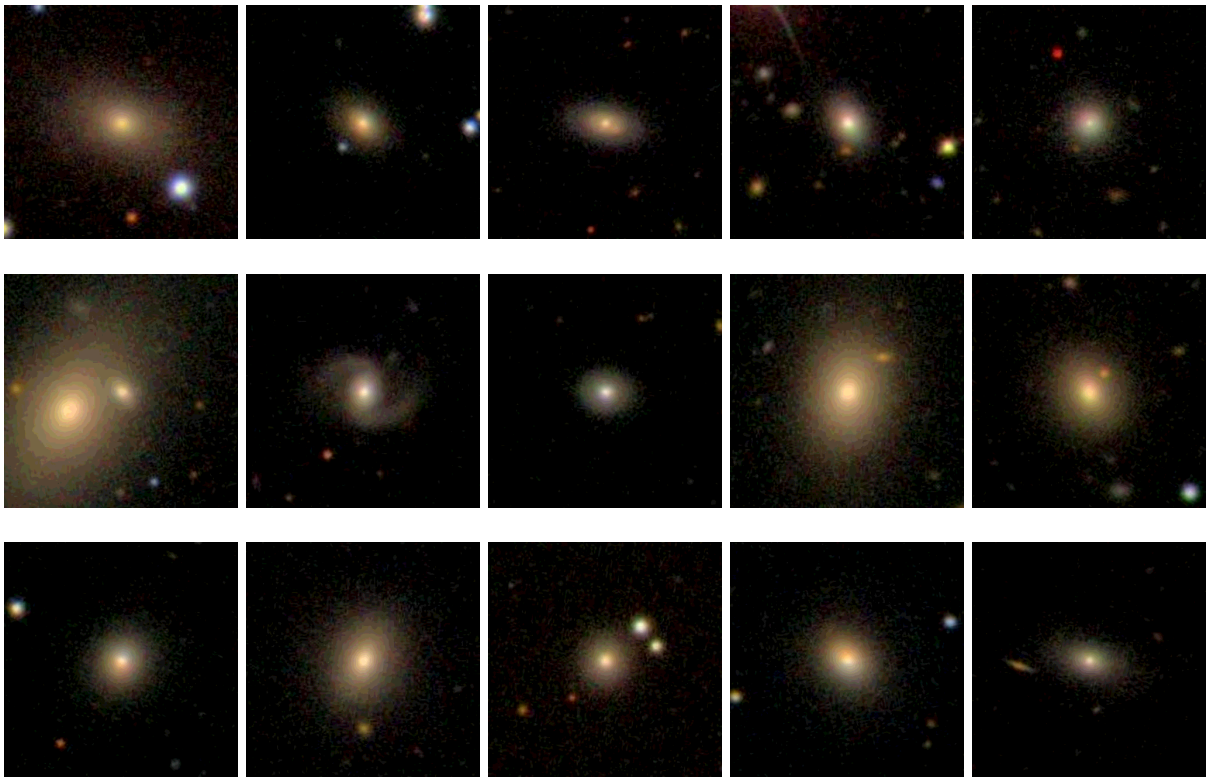

Figure 3: SDSS postage images of galaxies randomly selected from the *ETG sample*. The images are 1 arcminute square in size.

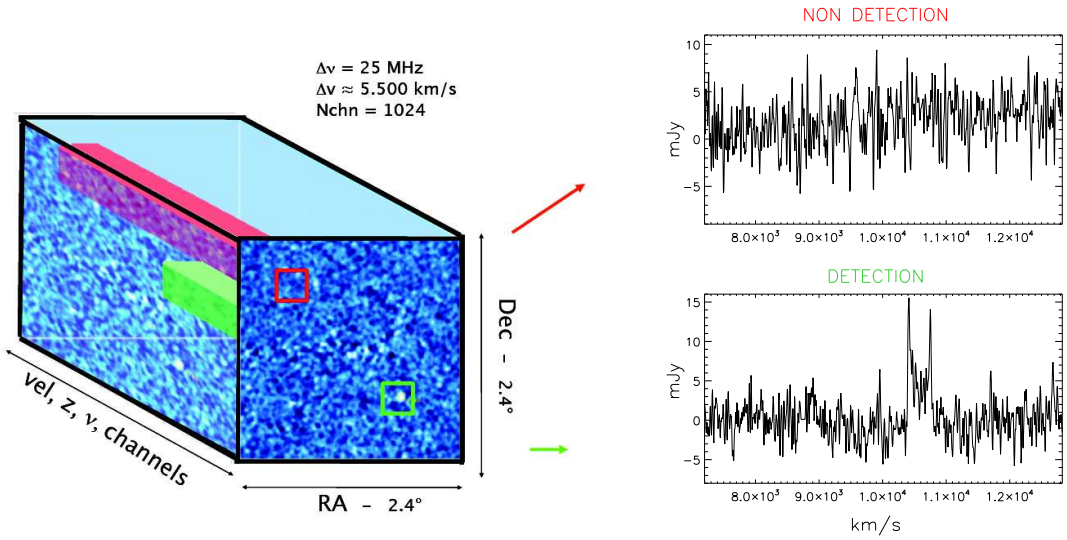

Figure 4: A schematic representation of an ALFALFA data-cube. The data cubes are $2.4^\circ \times 2.4^\circ$ in size and about 5500 km s^{-1} in velocity range (25 MHz in frequency). The average spectral resolution is $\sim$5.5 km s^{-1}; the spatial resolution is $4'$. For each pixel, which is a point in RA, Dec and velocity, a value of flux density is recorded. For each target in *sample A*, we extract a spectrum at a given position of the sky, over the velocity range of the data-cube which contains the source. Two examples of extracted spectra are shown on the right, illustrating a detection (green, bottom) and a non-detection (red,top).

sky and their redshifts. We select the ALFALFA data-cube which contains the target and integrate the signal from the galaxy over a sky region of $4' \times 4'$ (our GASS targets are always smaller then the Arecibo beam).
In Figure 4, we illustrate how we extract spectra at two different positions in the sky inside the same data-cube. The coloured regions indicate where the spectra would be evaluated.
For each spectrum we measure the root mean square (*rms*) noise.

b. Stacking spectra

We want to co-add the signals from N different sources located at different redshifts. First we shift each spectrum to the galaxy rest frequency, so each spectrum is centered at zero velocity. We stack together the spectra S_i (i=1,..N) using their $1/rms$ as a weight, so that the final spectrum S_{stack} is:

$$S_{stack} = \frac{\Sigma_{i=0}^{N} S_i \cdot w_i}{\Sigma_{i=0}^{N} w_i} \tag{3.1}$$

Figure 5 shows some examples of stacked spectra, obtained by stacking *sample A* galaxies in three different stellar mass intervals. In the left column of the Figure, we show spectra obtained by stacking ALFALFA detections and non-detections together. In the right panel we show the spectra obtained by stacking only the non-detections, demonstrating that the stacking process recovers a signal even if no individual galaxy is detected. Notice that the *rms* decreases with increasing number of co-added objects.

If we recover a signal in the stacked spectrum, we measure the integrated emission between the two edges of the HI profile, which are defined manually for each spectrum (dotted lines in Fig. 5). If there is no detection, we evaluate an upper limit, assuming a 5 σ signal with a width of 300 $\mathrm{km\,s^{-1}}$, smoothing the spectrum to 150 $\mathrm{km\,s^{-1}}$.

Evaluating HI gas fractions

Our aim is to characterize the average HI content of a given sample of galaxies, so we are interested in converting our recovered signal into an HI mass and also into an average HI gas fraction. Once we measure an HI flux, we can estimate an HI mass using the [12] formula:

$$\frac{M_{HI}}{\mathrm{M_\odot}} = \frac{2.356 \times 10^5}{1+z} \left(\frac{D_L(z)}{\mathrm{Mpc}}\right)^2 \left(\frac{S_{int}}{\mathrm{Jy\ km\ s^{-1}}}\right), \tag{3.2}$$

where $D_L(z)$ is the luminosity distance and S_{int} the integrated HI flux. A correction for HI self-absorption is not applied to the HI mass, as it is likely to be negligible. The HI gas fraction is simply defined as M_{HI}/M_*.

4. HI study of a complete sample of ETG galaxies

We ask whether bulge-dominated galaxies with $M_* > 10^{10} M_\odot$ lie on the same HI scaling relations as the general population of galaxies with $M_* > 10^{10} M_\odot$. Our goal is to determine whether the presence of the bulge plays a role in regulating the rate at which gas is consumed into stars, for example by stabilizing the disk (e.g., [13]). In order to test the role of the bulge in a clean way, we must account for the fact that the physical properties of galaxies are strongly correlated. It is therefore important to understand whether or not bulge-dominated galaxies differ in HI content from the parent sample at *fixed* values of these parameters.

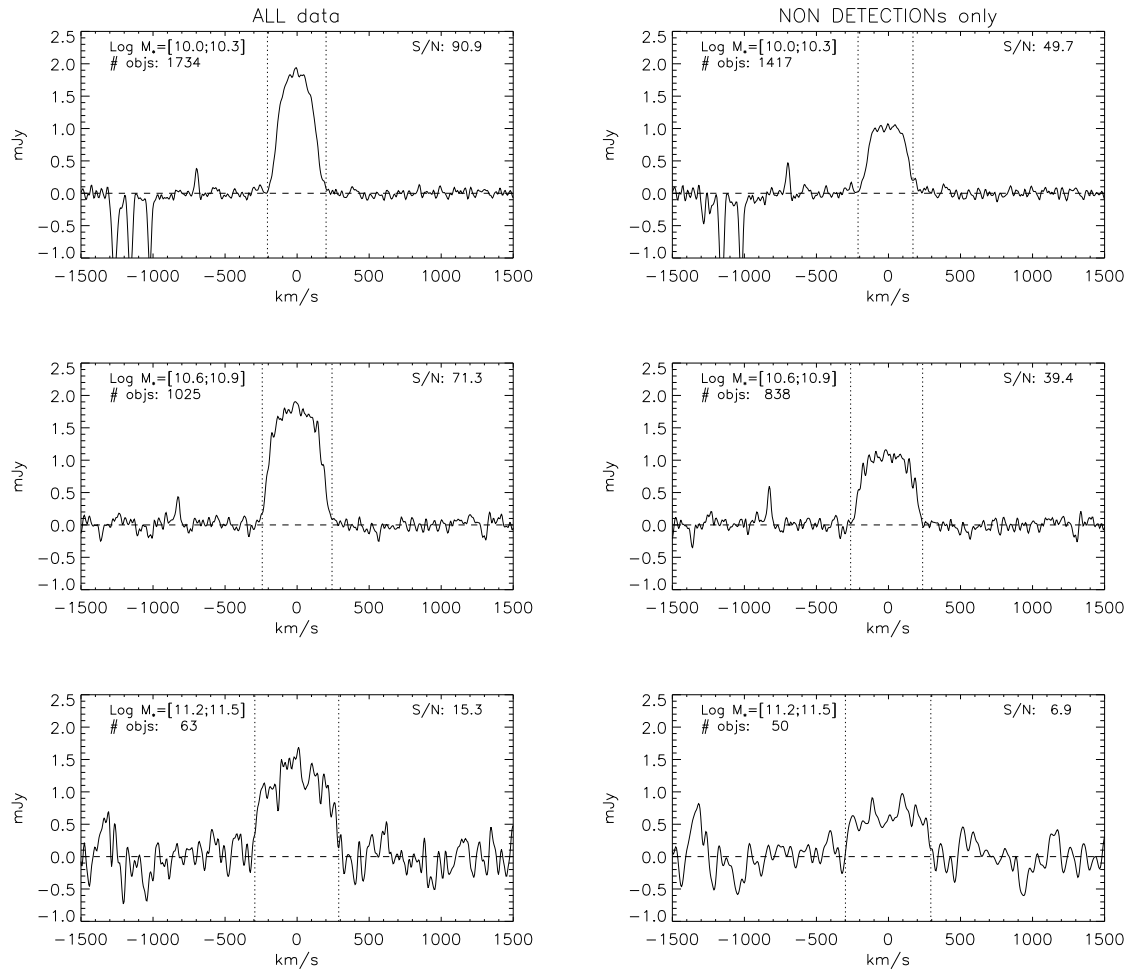

Figure 5: Examples of stacked spectra for three stellar mass bins. The x-axis is velocity in $\mathrm{km\,s^{-1}}$, the y-axis is HI flux density in mJy. For each spectrum, the mass range and the number of objects stacked are reported, as well as its signal-to-noise ratio. Dotted lines show the boundaries of the signal, inside which we integrate the flux. In some spectra there are spikes/holes caused by bad data (note that the spectra containing the bad data were not discarded because the bad pixels are located away from the central regions of interest). Left column: stacked spectra using all galaxies. Right column: stacked spectra using only those galaxies that were not detected by ALFALFA.

Our results are presented in Figure 6. In all the plots, blue circles are the average gas fractions obtained from stacking the *ETG sample* and the errorbars are evaluated using the *Jackknife method*. Upside-down triangles indicate the upper limit in the case of a stack that yields a non-detection. The red lines (circles) show the fits to the mean HI gas fraction relations obtained for *sample A*. Our main result is that the average HI gas fractions of bulge-dominated galaxies are significantly lower than those of the parent sample at a given value of stellar mass. A similar, but weaker reduction in the average HI gas fraction is seen for the *ETG sample* when it is plotted as a function of the central velocity dispersion of the bulge. However, the relation between gas fraction and stellar mass surface density and NUV-r colour appears to be insensitive to the ETG cut. In GASS-1 paper, Catinella et al. showed that a linear combination of stellar mass surface density and NUV-r colour

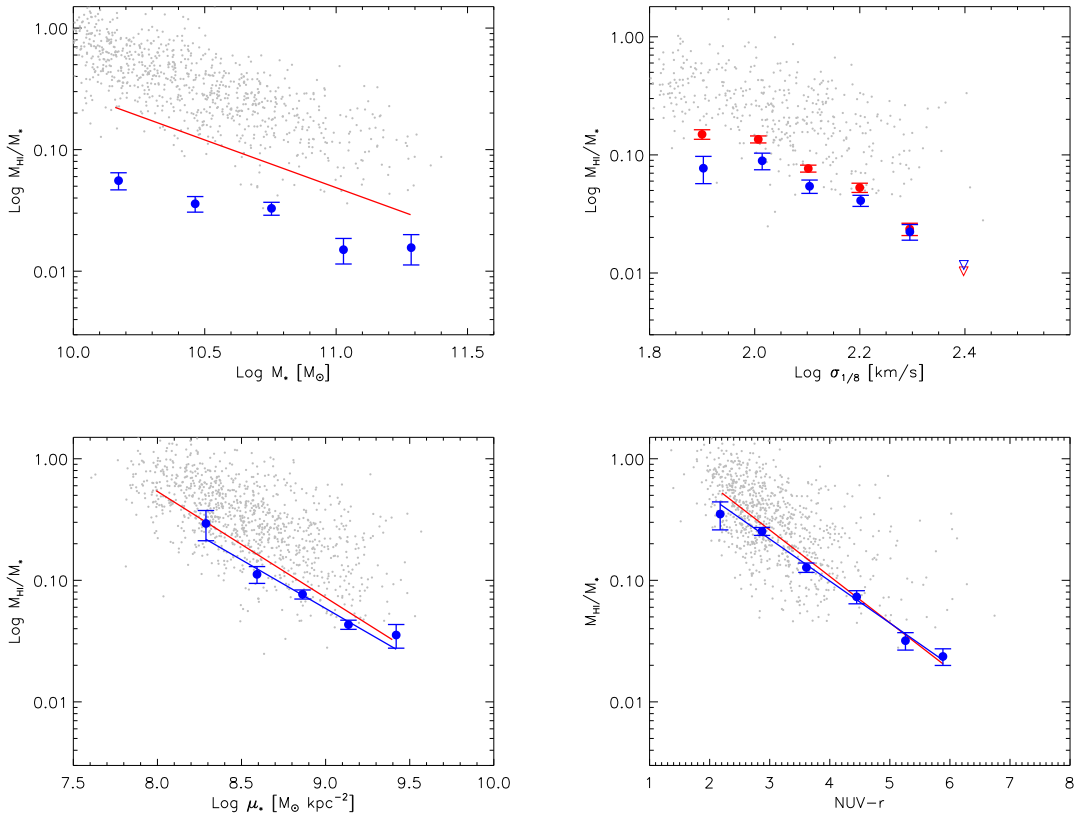

Figure 6: The dependence of the average HI gas fraction on stellar mass $M_\star$ (a), central velocity dispersion σ (b), stellar mass surface density $\mu_\star$ (c) and NUV$-r$ colour (d) for the *ETG sample* (blue symbols). The relations found for *sample A* are shown in red for comparison (the fit for the $M_\star$ relation, the actual points for σ). Upside-down triangles indicate upper limits in the case of a non-detection. Gray dots show *sample A* galaxies with ALFALFA detections.

provided an excellent way to "predict" the HI content of galaxies more massive than $10^{10}M_\odot$. Here we show that this conclusion holds true independent of the bulge-to-disk ratio of the galaxy.

In Figure 7, we show how the average gas fractions of galaxies in the *ETG sample* vary as a function of position in the two-dimensional plane of colour versus stellar mass density μ_* (We colour-code the (NUV$-r$)$-\mu_*$ plane according to gas fraction). Bulge-dominated galaxies are mainly found on the red sequence, but there is a minority population with bluer colours. The HI content decreases going from left to right (towards increasing stellar mass surface density) and from bottom to top (towards redder colours). The most significant variation is clearly along the colour direction, with little residual dependence on μ_*.

4.1 A Test of the morphological quenching scenario

The idea that galaxy disks are more resistant to the formation of bars, spiral density waves and other instabilities if they are embedded within a dynamically hot halo or bulge, has an early origin. Recently, [13] have proposed this so-called "morphological quenching" mechanism as a way of explaining why a disk with similar gas content will be much less efficient at forming stars if it is

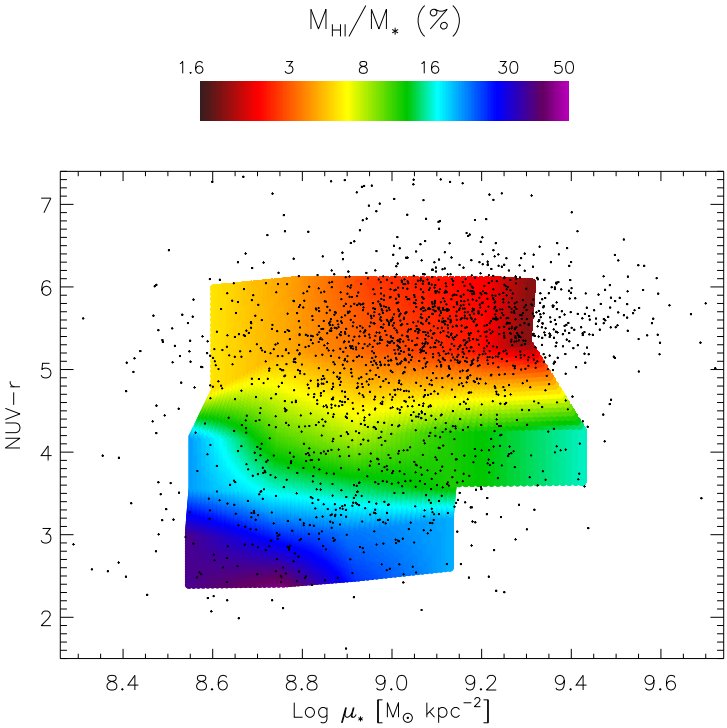

Figure 7: Average HI gas fraction dependence in the 2-dimensional plane of stellar mass surface density $\mu_\star$ and NUV$-r$ colour for galaxies in the *ETG sample*. The dots show individual objects, while the colors show the (interpolated) gas fractions measured with the stacking as a function of position in the plane (the colour scale key is included above the plot).

embedded in a galaxy with a significant bulge component. As stated in the abstract of their paper, "our mechanism automatically links the colour of the galaxy with its morphology, and does not require gas consumption, removal or termination of the gas supply."

To test whether the "morphological quenching" process is truly important in maintaining the low observed rates of star formation in red sequence galaxies, we have performed the following experiment. We have binned galaxies with $C < 2.6$ and $C > 2.6$ in the two-dimensional plane of NUV-r colour versus stellar mass (note that we use the same bin boundaries for both samples). We stack the HI spectra of the galaxies in each bin and calculate the average HI gas fraction, as explained above. In Figure 8, we report for each bin the ratio between the gas fraction of the disk-dominated objects and the bulge-dominated ones:

$$r = \left(\frac{M_{HI}}{M_*}\right)_{DD} / \left(\frac{M_{HI}}{M_*}\right)_{BD}$$

If the morphological quenching scenario is correct, then at fixed stellar mass, we would expect to find higher average HI gas fractions for bulge-dominated galaxies on the red sequence than for disk-dominated galaxies on the red sequence.

The results in Figure 8 show that in general the *opposite* is true. Gas fractions are always slightly higher for the disk-dominated galaxies than for bulge-dominated ones. The gas fraction differences do appear to be largest for red sequence galaxies with NUV-$r > 5$, but the sign of the

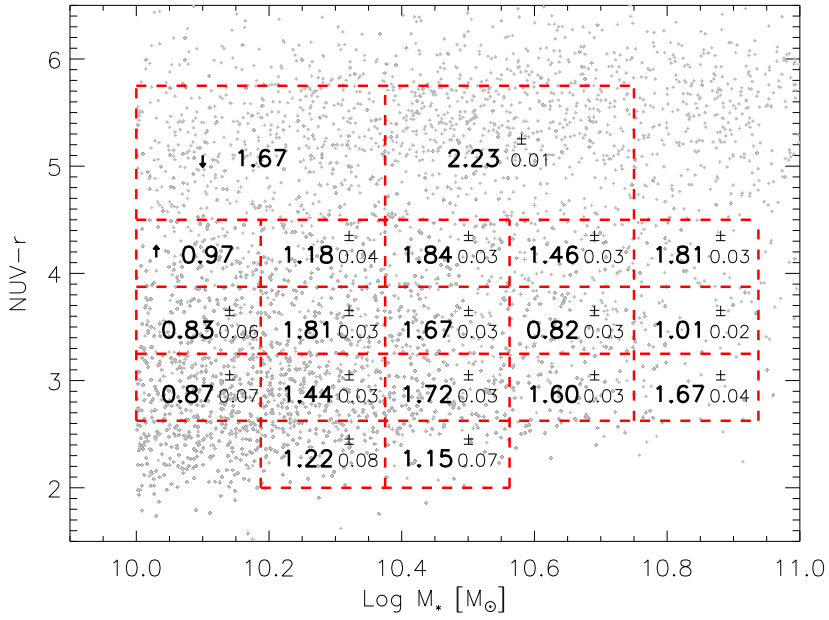

Figure 8: Morphological quenching test: for each bin of NUV$-r$ and $M_\star$ the ratio between the gas fractions of the disk-dominated galaxies with $C < 2.6$ and the bulge-dominated galaxies with $C > 2.6$ is reported. The arrows indicate upper/lower limit if one of the stacked spectra yielded a non-detection.

difference contradicts the predictions of Martig et al. (2009).
We note that these results are in agreement with those presented in [14]. In their paper, Schiminovich et al. use a volume-limited sample of 200 galaxies from the GASS survey to explore the global scaling relations associated with the ratio SFR/M_{HI}, which they call the *HI-based star formation efficiency*. They found that the average value of this star formation efficiency has little variation with any galaxy parameter, including the concentration index.

5. Summary

We have carried out a stacking analysis using ALFALFA scans of a volume-limited sample of ~ 5000 galaxies with imaging and spectroscopic data from GALEX and the Sloan Digital Sky Survey. The galaxies have stellar masses greater than $10^{10} M_\odot$ and redshifts in the range $0.025 < z < 0.05$. We extract a sub-sample of 1833 "early-type" galaxies with inclinations less than 70°, with concentration indices $C > 2.6$, and with light profiles that are well fit by a De Vaucouleurs model. We then stack the ALFALFA spectra of the galaxies from these two samples in bins of stellar mass, stellar mass surface density, central velocity dispersion, and NUV-r colour, and we use the stacked spectra to estimate the average HI gas fractions M_{HI}/M_* of the galaxies in each bin.

Our main result is that the HI gas fractions of both early-type and late-type galaxies correlate *primarily* with NUV-r colour and stellar mass surface density. The relation between average HI gas fraction and these two parameters is *independent* of C, and hence of the bulge-to-disk ratio of the galaxy. We note that at fixed stellar mass, early-type galaxies do have lower average HI fractions than late-type galaxies, but this effect arises because early-type galaxies are both smaller and redder

than late-type galaxies of the same stellar mass. The effect does not arise as a direct consequence of the presence of the bulge.

We have also tested whether the average HI gas content of bulge-dominated galaxies on the red sequence differs from that of late-type galaxies on the red sequence. We find no evidence that galaxies with a significant bulge component are less efficient at turning their available gas reservoirs into stars. This result is in contradiction with the "morphological quenching" scenario proposed by [13].

Further discussion and possible implications of this work will be discussed in [11].

References

[1] York, D. G., et al. 2000, *The Sloan Digital Sky Survey: Technical Summary*, *AJ* **120** (1579) 2000 [arXiv:astro-ph/0006396]

[2] Morganti, R., et al., *Neutral hydrogen in nearby elliptical and lenticular galaxies: the continuing formation of early-type galaxies*, *MNRAS* **371** (157) 2006 [arXiv:astro-ph/0606261]

[3] Giovanelli, R. et al., *The Arecibo Legacy Fast ALFA Survey. I. Science Goals, Survey Design, and Strategy*, *AJ* **130** (2598) 2005 [arXiv:astro-ph/0508301]

[4] Catinella B., et al., *The GALEX Arecibo SDSS Survey - I. Gas fraction scaling relations of massive galaxies and first data release*, *MNRAS* **403** (683) 2010 [arXiv:0912.1610] (GASS-1)

[5] Adelman-McCarthy J. K., et al., *The Sixth Data Release of the Sloan Digital Sky Survey*, *ApJ* **175** (297) 2008 [arXiv:0707.3413]

[6] Martin, D. C. et al., *The Galaxy Evolution Explorer: A Space Ultraviolet Survey Mission*, *ApJ* **619** (L1) 2005 [arXiv:astro-ph/0411302]

[7] Bernardi, M., et al., *Early-Type Galaxies in the Sloan Digital Sky Survey. I. The Sample*, *AJ* **125** (1817) 2003 [arXiv:astro-ph/0301631]

[8] Graves, G. J., Faber, S. M., & Schiavon, R. P., *Dissecting the Red Sequence. I. Star-Formation Histories of Quiescent Galaxies: The Color-Magnitude versus the Color-σ Relation*,*ApJ* **693** (486) 2009 [arXiv:0810.4334]

[9] Gadotti, D. A., *Structural properties of pseudo-bulges, classical bulges and elliptical galaxies: a Sloan Digital Sky Survey perspective*, *MNRAS* **393** (1531) 2009 [arXiv:0810.1953]

[10] Wang, J., Overzier, R., Kauffmann, G., von der Linden, A., & Kong, X., *The UV-optical colours of brightest cluster galaxies in optically and X-ray selected clusters*",*MNRAS* **401** (433) 2010 [arXiv:0909.1196]

[11] Fabello S., et al., *HI Properties of Galaxies from ALFALFA Data Stacking - I. Does the Bulge Quench Ongoing Star Formation?*, *MNRAS* submitted

[12] Roberts, M. S., *The Content of Galaxies: Stars and Gas*, *ARAA* **1** (149) 1963

[13] Martig, M., Bournaud, F., Teyssier, R., & Dekel, A., *Morphological Quenching of Star Formation: Making Early-Type Galaxies Red*", *ApJ* **707** (250) 2009 [arXiv:0905.4669]

[14] Schiminovich, D., et al., *The GALEX Arecibo SDSS Survey II: The Star Formation Efficiency of Massive Galaxies , MNRAS* 2010 arXiv:1006.5447